



Age-related alterations of articular cartilage in pituitary adenylate cyclase–activating polypeptide (PACAP) gene–deficient mice

Vince Szegezcki · Balázs Bauer · Adél Jüngling · Balázs Daniel Fülöp · Judit Vágó · Helga Perényi · Stefano Tarantini · Andrea Tamás · Róza Zákány · Dóra Reglődi · Tamás Juhász

Received: 25 June 2019 / Accepted: 22 August 2019 / Published online: 26 October 2019
© The Author(s) 2019

Abstract Pituitary adenylate cyclase activating polypeptide (PACAP) is an evolutionarily conserved neuropeptide which is produced by various neuronal and non-neuronal cells, including cartilage and bone cells. PACAP has trophic functions in tissue development, and it also plays a role in cellular and tissue aging. PACAP takes part in the regulation of chondrogenesis, which prevents insufficient cartilage formation caused by oxidative and mechanical stress. PACAP knockout (KO) mice have been shown to display early aging signs affecting several organs. In the present work, we investigated articular cartilage of knee joints in young and aged wild-type (WT) and PACAP KO mice. A significant increase in the thickness of articular cartilage was detected in aged PACAP gene–deficient mice. Amongst

PACAP receptors, dominantly PAC1 receptor was expressed in WT knee joints and a remarkable decrease was found in aged PACAP KO mice. Expression of PKA-regulated transcription factors, Sox5, Sox9 and CREB, decreased both in young and aged gene deficient mice, while Sox6, collagen type II and aggrecan expressions were elevated in young but were reduced in aged PACAP KO animals. Increased expression of hyaluronan (HA) synthases and HA-binding proteins was detected parallel with an elevated presence of HA in aged PACAP KO mice. Expression of bone related collagens (I and X) was augmented in young and aged animals. These results suggest that loss of PACAP signaling results in dysregulation of cartilage matrix composition and may transform articular cartilage in a way that it becomes more prone to degenerate.

Vince Szegezcki and Balázs Bauer; Dóra Reglődi and Tamás Juhász contributed equally to this work.

V. Szegezcki · B. Bauer · J. Vágó · H. Perényi · R. Zákány · T. Juhász (✉)
Department of Anatomy, Histology and Embryology, Faculty of Medicine, University of Debrecen, Nagyerdei krt. 98, Debrecen 4032, Hungary
e-mail: juhaszt@anat.med.unideb.hu

A. Jüngling · B. D. Fülöp · A. Tamás · D. Reglődi
Department of Anatomy, PTE-MTA PACAP Research Team, University of Pécs Medical School, Szigeti út 12, Pécs 7624, Hungary

S. Tarantini
Department of Geriatric Medicine, Reynolds Oklahoma Center on Aging, University of Oklahoma Health Sciences Center, Oklahoma City, OK, USA

Keywords Aggrecan · Collagen expression · Sox9 · Sox5 · Sox6 · Hyaluronic acid

Introduction

Articular cartilage is a unique type of connective tissue in the skeletal system with very poor regenerative capacity. Major factors behind this phenomenon are its avascular, aneural nature and the postmitotic character of adult chondrocytes. This tissue covers the articular surface of synovial joints providing frictionless gliding surface and shock absorption during locomotion (Redondo et al. 2018). High water content of the

extracellular matrix (ECM) and the specific collagen fibre orientation pattern is partly responsible for the resilience, weight bearing capacity and flexibility of the tissue (Redondo et al. 2018). In the superficial layer of articular cartilage, a proliferation zone can be identified, which has an important function in maintaining the elasticity of articular surface (Antons et al. 2018). Mature articular cartilage is composed of a specific ECM with dominantly collagen type II fibres, which run in a specific arcade-like orientation, and collagen type IX and XI associate to the core of the fibres in a healthy collagen network. The ground substance of cartilage ECM is rich in proteoglycans (PG) such as aggrecan (Laasanen et al. 2003). The glycosaminoglycan hyaluronic acid (HA) is another essential component of the ECM in articular cartilage as it forms a specific network with the PGs and binds high amounts of water. In the deep layers of articular cartilage (hypertrophic zone and calcification zone), ECM becomes calcified providing a tissue with intermediate biomechanical properties interconnecting articular cartilage and subchondral bone. In this region, chondrocytes are terminally differentiated hypertrophic cells which subsequently undergo apoptosis and the whole tissue serves as a template for trabecular bone formation (Zevenbergen et al. 2018). If any of the components mentioned above are downregulated or the balance in their expression is disturbed, cartilage homeostasis can become severely impaired (Li et al. 2018). In pathological conditions, such as inflammation, oxidative stress or increased mechanical force, the composition of cartilage-specific ECM can be disintegrated and cartilage degeneration may occur (Poulet and Staines 2016).

Secretion of cartilage-specific molecules is regulated by various signaling pathways in developing articular cartilage. Activation of PKA plays a crucial role in this process (Zakany et al. 2002) and can phosphorylate Sox9 or CREB transcription factors (Zakany et al. 2005). More active, phosphorylated forms of these transcription factors are transported to the nuclei and induce the expression of aggrecan and collagen type II. Inhibition of PKA leads to decreased cartilage formation (Zakany et al. 2001; Zakany et al. 2002) primarily via the lower activation of Sox9. Besides Sox9, other members of the SoxE family can also be activated in cartilage formation such as Sox5 and Sox6 (Liu and Lefebvre 2015). Alterations in the expression of the latter two transcription factors leads to a modified, pathologically deformed skeleton and impaired cartilage formation

(Lefebvre et al. 2001). Although protein kinase A (PKA) is a key regulator in cartilage formation or regeneration, several other pathways have also been shown to participate. The importance of hedgehog (HH) (Juhasz et al. 2015b), ERK (Zakany et al. 2005) or protein kinase C (PKC) signaling (Matta et al. 2011) is unquestionable. Certain members of the Ser/Thr phosphatases such as protein phosphatase 2A (PP2A) (Zakany et al. 2001) and PP2B (Zakany et al. 2005) are also proven to play a regulatory role in proper cartilage formation. Although the regulatory factors in chondroprogenitor cell differentiations are being characterized, there are still numerous signaling connections not clarified. Amongst these, pituitary adenylate cyclase activating polypeptide (PACAP) is a recently identified player.

PACAP was identified and isolated from the central nervous system (CNS) by Miyata et al. (1989). It has two biologically active forms, PACAP 1-38 and PACAP 1-27, which are evolutionarily well conserved (Vaudry et al. 2009). The neuropeptides have three major G protein coupled receptors, namely PAC1, VPAC1 and VPAC2. PAC1 receptor has the highest affinity to the neuropeptide, and the activation of the receptor triggers adenylate cyclase activity leading to increased concentration of intracellular cAMP and ultimately activates PKA signaling (Gourlet et al. 1997). A positive role of PACAP has been shown in *in vitro* cartilage formation (Juhasz et al. 2014a), and its protective role has been proven against oxidative stress (Juhasz et al. 2015a; Juhasz et al. 2014a) and mechanical force induced damage (Juhasz et al. 2015b; Szenteleky et al. 2019). Furthermore, PACAP receptor expression has been shown in osteoarthritic cartilage (Giunta et al. 2015), and a pivotal function of PACAP has also been demonstrated in bone formation (Jozsa et al. 2018; Juhasz et al. 2014b). Differentiation of other peripheral cells and organs can be related to proper PACAP signaling such as development of sperms (Reglodi et al. 2018c), teeth (Fulop et al. 2018; Sandor et al. 2014) and brain (Vaudry et al. 2009). On the other hand, lack of PACAP influences aging processes in different tissues (Reglodi et al. 2018b) and is related to accumulation of amyloid deposits (Reglodi et al. 2018b). Lack of the neuropeptide also modulates the vasomotor response of arteries (Ivic et al. 2017) and retina functions (Kovacs-Valasek et al. 2017) during aging.

Although there are some studies on PACAP in aging, no experimental data is available on the regulation of

cartilage aging. Cells of the hyaline cartilage have extremely long lifespan but little is known about their signaling alterations in aging. As accelerated aging has been demonstrated in PACAP gene-deficient mice, we investigated the in vivo signaling alterations in young and aged wild-type (WT) and PACAP knock out (KO) mice.

Materials and methods

Animals

Generation and maintenance of the PACAP-deficient mice on the CD1 background have been described in detail (Hashimoto et al. 2001). They were backcrossed for at least ten generations with the CD1 strain. Genotype was tested with PCR reactions. For the experiments, we sacrificed 3-month-old (“young”) and 1-year-old (“aged”) wild-type (WT, $n = 20$ – 20) and homozygous PACAP-deficient (PACAP KO, $n = 20$ – 20) mice. Animals were fed and watered ad libitum, under light/dark cycles of 12/12 h. Hind limbs were removed after sacrificing the mice with an overdose of pentobarbital sodium (100 mg/kg bw). All procedures were performed in accordance with the ethical guidelines approved by the University of Pécs (permission number: BA02/2000-15024/2011).

Staining procedure

Knee joints were dissected, and after additional tissues were removed, samples were washed in PBS three times and fixed in a 4:1 mixture of absolute ethanol and 40% formaldehyde. Joints were decalcified in 4% EDTA for 4 weeks until bones became soft. Then samples were dehydrated in ascending alcohol row and embedded in paraffin. Five-micrometre-thick serial sections were made. After rehydration haematoxylin-eosin (HE) (Sigma-Aldrich, MO, USA) and dimethylmethylene blue (DMMB) (Sigma-Aldrich, MO, USA), stainings were performed. All staining protocols were carried out according to the instructions of manufacturer. Photomicrographs were taken using DP74 camera (Olympus Corporation, Tokyo, Japan) on Olympus Bx53 microscope (Olympus Corporation, Tokyo, Japan).

Cartilage thickness measurement

Measurement of mean thickness of cartilage on a convex segment

For the measurement of articular cartilage thickness, a customized mathematical formula was used. A circular arc that best fits to the surface of the cartilage was constructed in *Adobe Illustrator 19.0.0* (Adobe Inc., San Jose, CA, USA) with the help of the SubScribe plug-in (Astute Graphics Limited, UK). Two arbitrary perpendicular lines (radiuses, r) were then drawn from this arc, defining the α angle and the segment of the cartilage used for the measurement. Both α and r were measured in pixels in *Adobe Illustrator*. Length of the scale bar was measured as well for calculating the conversion ratio from pixels to micrometres (Fig. 1a). Area of the bound segment of the cartilage was measured using the ImageJ 1.40 g freeware freehand selection tool. Thickness (\bar{l}) was defined as the difference of the radius of the outer and inner circles of an annulus that had an outer arc conforming to the surface of the cartilage and the area of which equals that of the portion of cartilage bound by the radiuses. Thus, A was the area of the annulus sector of angle α and was calculated as follows:

$$A = A_r - A_{r-\bar{l}}$$

$$A = r^2 \pi \frac{\alpha}{360^\circ} - (r - \bar{l})^2 \pi \frac{\alpha}{360^\circ}$$

$$0 = \bar{l}^2 \pi \frac{\alpha}{360^\circ} - 2r\bar{l}\pi \frac{\alpha}{360^\circ} + A$$

$$a = \pi \frac{\alpha}{360^\circ}, b = -2r\pi \frac{\alpha}{360^\circ}, c = A.$$

After rearranging and solving the quadratic equation for \bar{l} , the thickness of the cartilage is converted to micrometres.

Measurement of mean thickness of cartilage on a concave segment

Essentially, the same process was carried out, with some changes made to the equation (Fig. 1b).

$$A = A_{r+\bar{l}} - A_r$$

$$A = (r + \bar{l})^2 \pi \frac{\alpha}{360^\circ} - r^2 \pi \frac{\alpha}{360^\circ}$$

$$0 = \bar{l}^2 \pi \frac{\alpha}{360^\circ} + 2r\bar{l}\pi \frac{\alpha}{360^\circ} - A$$

$$a = \pi \frac{\alpha}{360^\circ}, b = 2r\pi \frac{\alpha}{360^\circ}, c = -A$$

Measuring mean thickness of cartilage on a straight segment

Thickness (\bar{l}) was the height of the rectangle that had an area equal to that of and the same width (x) as the selected segment of cartilage (Fig. 1c).

$$A = x\bar{l}$$

$$\bar{l} = \frac{A}{x}$$

Immunohistochemistry

Knee joints were dissected, and additional tissues were removed. Joints were washed in PBS three times and fixed in a 4:1 mixture of absolute ethanol and 40% formaldehyde for 24 h. Joints were decalcified in 4% EDTA for 4 weeks until bones became soft. Then, samples were dehydrated in graded ethanol series and embedded in paraffin. Five micrometres of serial sections were made. Sections were rehydrated in descending alcohol row and washed in PBST (phosphate-buffered saline supplemented with 1% Tween-20) three times. Nonspecific binding sites were blocked in PBST supplemented with 1% bovine serum albumin (BSA, Amresco LLC, Solon, OH, USA) at 37 °C for 30 min in a humidified-chamber.

For collagen typeX detection, a monoclonal anti-collagen type X (Sigma-Aldrich, MO, USA) at a dilution of 1:500 was used at 4 °C overnight. Primary antibody was visualized with anti-mouse Alexa555 secondary antibody (Life Technologies Corporation,

Carlsbad, CA, USA) at a dilution of 1:1000. Slides were mounted in Vectashield Hard Set mounting medium (Vector Laboratories, Peterborough, England).

Hyaluronic acid (HA) was detected by using a biotinylated HA-binding complex in 5 µg/mL concentration (bHABC, kindly provided by R. Tammi and M. Tammi, Department of Anatomy, University of Kuopio, Kuopio, Finland) at 4 °C overnight. The reaction was visualized with Streptavidin-Alexa555 (2 µg/mL, Invitrogen Corporation, Carlsbad, CA, USA) for fluorescence microscopy. Tissues were mounted in Vectashield Hard Set mounting medium (Vector Laboratories, Ltd. Peterborough, UK).

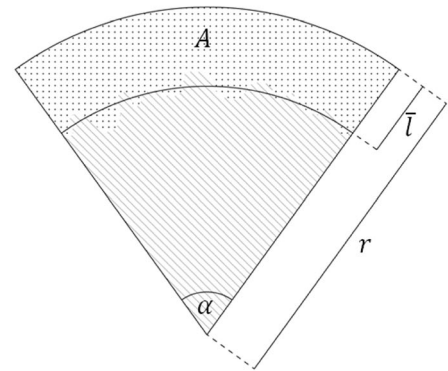
Photomicrographs of collagen type X immunohistochemistry were taken using an Olympus DP72 camera on a Nikon Eclipse E800 microscope (Nikon Corporation, Tokyo, Japan). Images were acquired using cellSense Entry 1.5 software (Olympus, Shinjuku, Tokyo, Japan) with constant camera settings to allow comparison of fluorescent signal intensities. Images of Alexa555 were overlaid using Adobe Photoshop version 10.0 software.

RT-PCR analysis

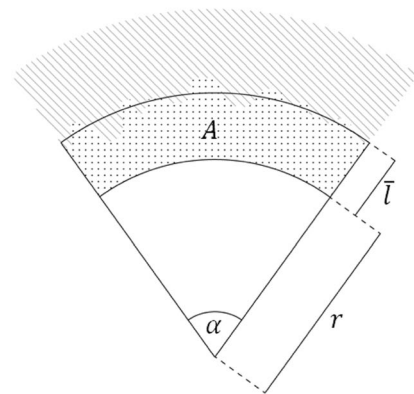
Articular cartilage from knee joints was isolated under microscope, and samples were kept in RNAlater (Sigma-Aldrich MO, USA). Tissues were cryo-ground in liquid nitrogen and dissolved in Trizol (Applied Biosystems, Foster City, CA, USA) and kept at −70 °C for 24 h, and after the addition of 20% RNase-free chloroform, samples were centrifuged at 4 °C at 10,000×g for 15 min. Samples were incubated in 500 µL of RNase-free isopropanol at −20 °C for 1 h; then, total RNA was harvested in RNase free water and stored at −20 °C. The assay mixture for reverse transcriptase reaction contained 2 µg RNA, 0.112 µM oligo(dT), 0.5 mM dNTP and 200 units of High Capacity RT (Applied Biosystems, Foster City, CA, USA) in 1× RT buffer. For the sequences of primer pairs and further details of polymerase chain reactions, see Table 1. Amplifications were performed in a thermal cycler (Labnet MultiGene™ 96-well Gradient Thermal Cycler; Labnet International, Edison, NJ, USA) in a final volume of 11 µL (containing 1 µL forward and reverse primers [0.4 µM], 0.5 µL dNTP [200 µM], and 5 units of Promega GoTaq® DNA polymerase in 1× reaction buffer) as follows: 95 °C, 2 min,

Fig. 1 Measurement of mean thickness of cartilage. Convex segment (a): the mean thickness (\bar{l}) of the cartilage (dotted area) is the difference of the outer and inner radius of the annulus segment that has an area equal to the area (A) of the cartilage segment of the same α angle. Mean thickness can be calculated with the formula for the area of an annulus segment. The striped area represents subchondral bone. r —outer radius of the constructed annulus segment. Concave segment (b): measuring the thickness of cartilage on a concave segment. Dotted and striped areas represent cartilage and subchondral bone, respectively. A —area of the cartilage segment of α , \bar{l} —mean thickness, r —inner radius of the constructed annulus segment. Straight segment (c): measuring the thickness of cartilage on a straight segment. Dotted and striped areas represent cartilage and subchondral bone, respectively. A —area of the cartilage segment, \bar{l} —mean thickness, x —width of the constructed rectangle and the selected segment of cartilage

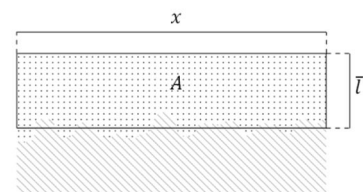
a Thickness of cartilage on a convex area



b Thickness of cartilage on a concave segment



c Thickness of cartilage on a straight segment



followed by 35 cycles (denaturation, 94 °C, 1 min; annealing at optimized temperatures as given in Table 1 for 1 min; extension, 72 °C, 90 s) and then 72 °C, 10 min. PCR products were analysed by electrophoresis in 1.2% agarose gel containing ethidium bromide. Actin was used as internal control. Optical density of signals was measured by using ImageJ 1.40 g freeware, and results were normalized to the optical density of control tissue.

Western blot analysis

Articular cartilage of knee joints was removed under microscope and was kept in 100 μ L of homogenization RIPA. Tissues were cryo-ground in liquid nitrogen. After centrifugation, tissue pellets were suspended in 100 μ L of homogenization RIPA and samples were stored at -70 °C. Suspensions were sonicated by pulsing burst for 30 s at 40 A (Cole-Parmer, IL, USA). For

setting equal protein concentration, BCA protein assay was used (Pierce™, MA, USA) and Laemmli electrophoresis sample buffer (4% SDS, 10% 2-mercaptoethanol, 20% glycerol, 0.004% bromophenol blue, 0.125 M TrisHCl pH 6.8) was added to cell lysates and boiled for 10 min. About 10 µg of protein was separated by 7.5% SDS-PAGE gel for detection of PAC1, VPAC1, VPAC2, PKA, CREB, P-CREB, Sox9, P-Sox9, Sox5, Sox6, collagen type I, collagen type X, Chst11, HAS2, HAS3, RHAMM, HAPLN1, and CD44 and by 5% SDS-PAGE gel for detection collagen type II and aggrecan. Proteins were transferred electrophoretically to nitrocellulose membranes with TransTurbo blot (Bio-Rad Laboratories, CA, USA) in 10 min. After blocking with 5% non-fat dry milk in phosphate-buffered saline (PBST) with 0.1% Tween 20, membranes were washed and exposed to the primary antibodies overnight at 4 °C in the dilution as given in Table 2. After washing for 30 min in PBST, membranes were incubated with anti-rabbit IgG (Bio-Rad Laboratories, CA, USA) in 1:1500 and anti-mouse IgG (Bio-Rad Laboratories, CA, USA) in 1:1500 dilution. Signals were detected by enhanced chemiluminescence (Advansta Inc., San Jose, CA, USA) according to the instructions of the manufacturer and documented by gel documentary system (Fluorchem E, ProteinSimple, CA, USA). Optical density of Western blot signals was measured by using ImageJ 1.40g freeware, and results were normalized to that of control samples.

Statistical analysis

All data are representative of at least five independent experiments. Where applicable, data are expressed as mean ± SEM. Statistical analysis was performed by Student's *t* test. Threshold for statistically significant differences as compared to respective control (wild-type animals) was set at **p* < 0.05.

Results

Thickness of articular cartilage increased in aged PACAP gene-deficient mice

DMMB staining was performed to demonstrate the presence of metachromatic ECM components (PGs, sulphated GAGs). There was similar metachromasia in young WT and PACAP gene-deficient mice, while metachromasia

was paler in aged KO cartilage (Fig. 2a). No significant macroscopic alterations were detected in the morphology of young WT or PACAP KO articular cartilage with HE staining. Furthermore, morphologically, no differences were visible in the articular cartilage of knee joints in aged WT or PACAP gene-deficient mice (Fig. 2b). Thickness of articular cartilage was measured with a mathematical geometric method in 10 different joints both in tibial and femoral articular cartilages. In young PACAP animals, cartilage was tendentiously thicker but no significant alterations were measured compared with WT mice (Fig. 2c). On the contrary, significantly thicker cartilage was detected in aged PACAP KO mice compared with aged WT animals (Fig. 2c).

PACAP receptors diminished in aged cartilage of PACAP KO mice

As PACAP can act on three different receptors, we monitored mRNA and protein expressions of PAC1, VPAC1 and VPAC2 receptors in articular cartilage. In young animals, only WT cartilage showed PACAP expression as it was expected (Fig. 3a). On the other hand, no preproPACAP expression was detected in aged WT or PACAP KO animals (Fig. 3a). Expression of the main PACAP-binding receptor, PAC1, was detected in WT and PACAP gene-deficient young animals with equal expression (Fig. 3a, b). In aged cartilage, no PAC1 receptor mRNA or protein expression was detected (Fig. 3a, b). Moreover, VPAC1 expression was similar to PAC1 with an absence in aged PACAP gene-deficient mice (Fig. 3a, b), while VPAC2 was not detectable in hyaline cartilage.

Expression of canonical PACAP downstream signaling molecules altered in PACAP gene-deficient animals

Next, classical downstream targets of PACAP binding were investigated. Both the mRNA and protein expressions of PKA were reduced in young PACAP KO cartilages (Fig. 4a, b). Moreover, in aged PACAP, gene-deficient cartilage protein expression of PKA was hardly detectable with this method (Fig. 4a, b). CREB mRNA and protein expressions did not significantly change in young PACAP KO articular cartilage but its phosphorylated, more active form decreased in aged cartilage. The mRNA and protein expressions of CREB and the protein expression of P-CREB were reduced (Fig. 4a, b). Next, expression of SoxE family members

Table 1 Nucleotide sequences, amplification sites, GenBank accession numbers, amplicon sizes and PCR reaction conditions for each primer pair are shown

Gene	Primer	Nucleotide sequence (5' → 3')	GenBank ID	Annealing temperature (°C)	Amplicon size (bp)
preproPACAP	Sense	GAA GAC GAG GCT TAC GAC CA (314–333)	NM_001315503.1	58	288
	Antisense	GTC CGA GTG GCG TTT GGT (584–601)			
PAC1	Sense	TATTACTACCTGTCGGTGAAG(912–932)	NM_007407.4	52	213
	Antisense	ATGACTGCTGCTCTGCTC (1107–1124)			
VPAC1	Sense	TTT GAG GAT TTC GGG TGC (974–991)	NM_011703.4	53	266
	Antisense	TGG GCC TTA AAG TTG TCG (1222–1239)			
VPAC2	Sense	CTC CTG GTA GCC ATC CTT (805–822)	NM_009511.2	53	149
	Antisense	ATG CTG TGG TCG TTT GTG (936–953)			
PKA (Prkaca)	Sense	GCAAAGGCTACAACAAGGC (847–865)	NM_008854	53	280
	Antisense	ATGGCAATCCAGTCAATCG (1109–1126)			
CREB (Creb1)	Sense	AGATTGCCACATTAGCCC (95–112)	NM_031017.1	52	441
	Antisense	GCTGTATTGCTCCTCCCT (518–535)			
Sox9	Sense	GTA CCC GCA TCT GCA CAA CG (378–397)	NM_011448	62	521
	Antisense	GTG GCA AGT ATT GGT CAA ACT CAT T (874–898)			
Sox6	Sense	GGG GTC GGG AGC GTG AAA (483–500)	NM_001277326.1	54	381
	Antisense	GGC GAG CAA GGT CCA TTT (846–863)			
Sox5	Sense	GCT CCA TAC AAC TCA TCT AC (504–523)	NM_011444.3	53	181
	Antisense	TGT CTT CTG GCT CAT TCT (667–684)			
Aggrecan	Sense	CGG GAA GGT TGC TAT GGT G (782–800)	NM_007424.2	59	359
	Antisense	CCT GTC TGG TTG GCG TGT A (1122–1140)			
Col2a1	Sense	AAA GAC GGT GAG ACG GGA GC (1900–1919)	NM_001113515	63	289
	Antisense	GAC CAT CAG TAC CAG GAG TGC C (2167–2188)			
Chst11	Sense	TGC TAT GTG CCC AAG GTA (822–839)	NM_021439.2	55	466
	Antisense	CGA GGT CGT AGT GGA TGTG (1269–1287)			
HAS2	Sense	ACAGGCATCTCACGAACC (1479–1496)	NM_008216.3	51	415
	Antisense	ATC TTG GCG GGA AGT AAA (1876–2893)			
HAS3	Sense	TCGCGGATTTCGGTGGACT (835–852)	NM_001331048.1	59	280
	Antisense	TGCTGGAGGAGGCTGTTGC (1096–1114)			
HAPLN1	Sense	GGC TCA GGA ATC CAC AAA (217–234)	BC066853	55	284
	Antisense	GGA AAG TAA GGG AAC ACC A (482–500)			
RHAMM	Sense	GAG GGA CTC AGG ACA AAC (374–391)	NM_013552.2	49	485
	Antisense	TTC TTC TAA CTG GGC AAT (8412–858)			
CD44	Sense	GGATTCATCCCAACGCTAT (600–618)	NM_009851.2	53	216
	Antisense	ACT CGC CCT TCT TGC TGT (798–815)			
Col1a1	Sense	GGG CGA GTG CTG TGC TTT (237–254)	BC050014	62	388
	Antisense	GGG ACC CAT TGG ACC TGA A (606–624)			
Col10a1	Sense	TTC TGG GAT GCC GCT TGT C (1602–1620)	NM_009925	61	263
	Antisense	TCG TAG GCG TGC CGT TCT T (1846–1864)			
Actin (Actb)	Sense	GCCAACCGTGAAAAGATGA (419–437)	NM_007393.5	54	462
	Antisense	CAAGAAGGAAGGCTGGAAAA (861–880)			

followed. In young cartilage, the mRNA expression of Sox9 was significantly elevated, while a significant decrease was detected in Sox9 and P-Sox9 protein

expressions (Fig. 4a, b). Analysis of Sox6 expression showed an unexpected result. In young PACAP KO animals elevated mRNA and protein expressions of

Table 2 Table of antibodies used in the experiments

Antibody	Host animal	Dilution	Distributor
Anti-PAC1	Rabbit, polyclonal	1:600	Sigma-Aldrich, St. Louis, MO, USA
Anti-VPAC1	Rabbit, polyclonal	1:800	Alomone Labs., Jerusalem, Israel
Anti-VPAC2	Rabbit, polyclonal	1:600	Abcam, Cambridge, UK
Anti-Coll. I.	Mouse, monoclonal	1:1000	Sigma-Aldrich, St. Louis, MO, USA
Anti-CREB	Rabbit, polyclonal	1:800	Millipore, Billerica, MA, USA
Anti-P-CREB	Rabbit, polyclonal	1:800	Millipore, Billerica, MA, USA
Anti-Coll. II.	Mouse, monoclonal	1:500	Novus Biologicals, Littleton, CO, USA
Anti-HAS2	Rabbit, polyclonal	1:300	Santa Cruz Biotechnology Inc., Santa Cruz, CA, USA
Anti-HAS3	Rabbit, polyclonal	1:300	Sigma-Aldrich, St. Louis, MO, USA
Anti-Coll. X.	Rabbit, polyclonal	1:500	Sigma-Aldrich, St. Louis, MO, USA
Anti-Sox9	Rabbit, polyclonal	1:600	Abcam, Cambridge, UK
Anti-P-Sox9	Rabbit, polyclonal	1:800	Sigma-Aldrich, St. Louis, MO, USA
Anti-PKA	Rabbit, polyclonal	1:800	Cell Signaling, Danvers, MA, USA
Anti-RHAMM	Mouse, monoclonal	1:500	Novocastra Laboratories Ltd., Newcastle, UK
Anti-Aggregan	Rabbit, polyclonal	1:600	Millipore, Billerica, MA, USA
Anti-HAPLN1	Mouse, monoclonal	1:500	R&D Systems, Minneapolis, MN, USA
Anti-Chst11	Rabbit, polyclonal	1:600	Sigma-Aldrich, St. Louis, MO, USA
Anti-CD44	Mouse, polyclonal	1:800	R&D Systems, Minneapolis, MN, USA
Anti-Sox5	Rabbit, polyclonal	1:500	Abcam, Cambridge, UK
Anti-Sox6	Rabbit, polyclonal	1:500	Abcam, Cambridge, UK
Anti-actin	Mouse, monoclonal	1:10000	Sigma-Aldrich, St. Louis, MO, USA

Sox6 were detected (Fig. 4a, b), while Sox6 protein became undetectable in aged PACAP gene-deficient mice (Fig. 4a, b). Finally, Sox5 mRNA and protein expressions significantly decreased in young PACAP KO cartilage and no expression was detected in old WT and PACAP KO mice (Fig. 4a, b).

Alterations of ECM production in PACAP KO mice

In further steps, effects of PACAP and aging were monitored in production of cartilage specific ECM. Aggrecan, the main proteoglycan of hyaline cartilage showed an elevated mRNA and protein expression in young PACAP gene-deficient mice (Fig. 5a, b). On the contrary, both the mRNA and protein expressions were reduced in aged PACAP KO mice (Fig. 5a, b). Interestingly, the mRNA expression of collagen type II was diminished, but increased protein expression was detected in young PACAP KO cartilage (Fig. 5a, b). In aged PACAP gene-deficient mice, both the mRNA and protein expressions of collagen type II were decreased (Fig. 5a, b). Chst11 catalyses the transfer of sulphate to chondroitin. Both the mRNA and

protein expressions of this transferase decreased in young and aged PACAP gene-deficient articular cartilage (Fig. 5a, b). HAPLN1 (link protein) can stabilize the aggregates of aggrecan monomers with HA and helps with the formation of the cartilage specific ECM network. Similarly to aggrecan core, protein expression HAPLN1 showed an increased expression in young PACAP KO animals but it reduced during aging (Fig. 5a, b). Production of HA in cartilage is regulated by two hyaluronan synthases, HAS2 and HAS3. Interestingly, the mRNA and the protein expressions of these enzymes elevated in both young and aged PACAP KO mice (Fig. 5a, b). Binding of HA can occur intracellularly by RHAMM or on the cell surface by CD44. mRNA and protein expressions of RHAMM and CD44 were elevated in young PACAP gene-deficient mice (Fig. 5a, b). On the contrary, RHAMM expression decreased in aged PACAP KO mice. CD44 protein expression similarly to HAS enzymes elevated in aged PACAP gene-deficient animals (Fig. 5a, b).

HA content of articular cartilage was also investigated, and high amount of GAG was visible around the chondrons of WT articular cartilage (Fig. 5c). The

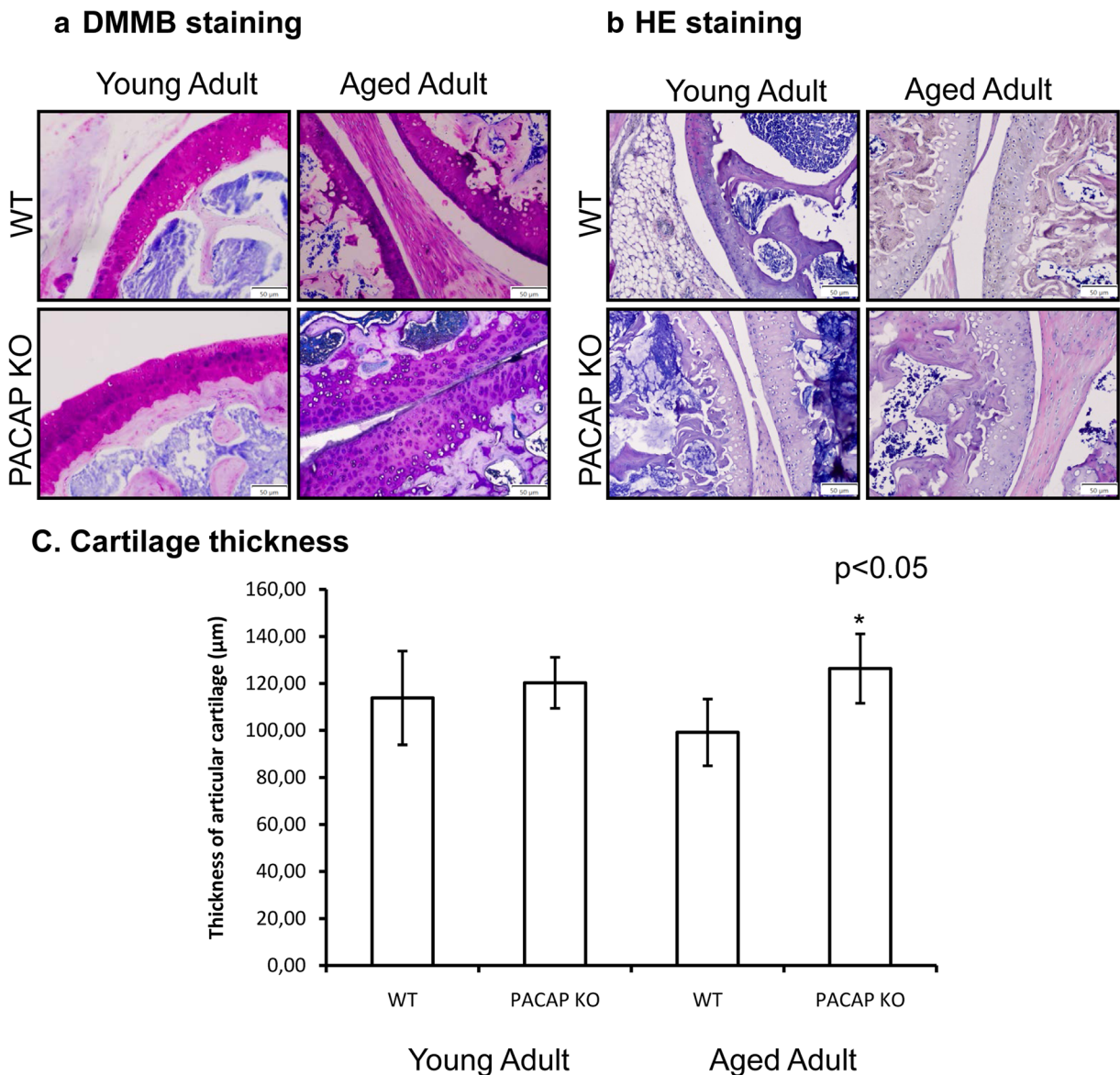


Fig. 2 Morphological analysis of knee joints of young and aged WT and PACAP KO mice. Dimethylmethylene blue (DMMB) (a) and hematoxylin-eosin (HE) staining (b) were used to visualize the histological differences. Original magnification was $\times 20$. Scale

bar: 50 μm . Geometric analysis (c) of mouse articular cartilage. Representative data of 10 independent experiments. Asterisks indicate significant ($*p < 0.05$) difference in thickness of cartilage compared to the respective control

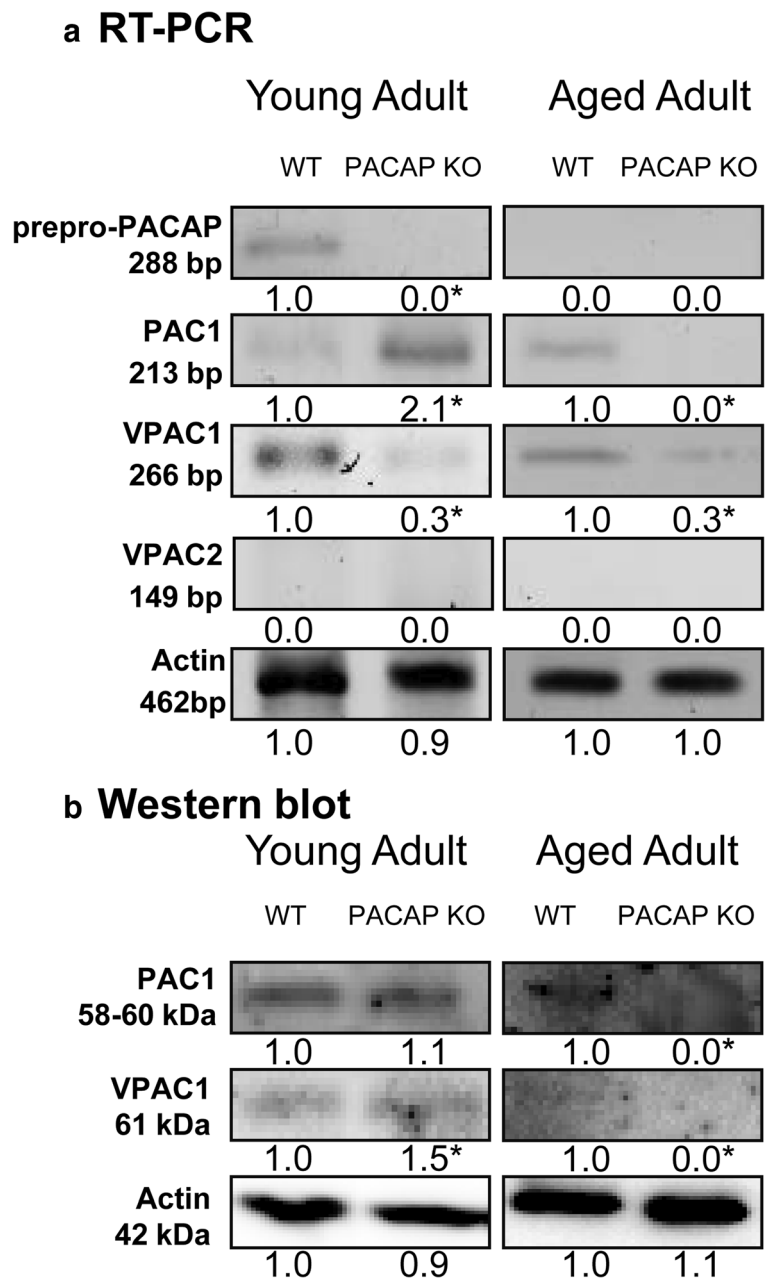
amount of HA was increased both in young and aged PACAP gene-deficient mice (Fig. 5c).

Bone-specific collagens accumulated in PACAP KO cartilage in aging

Furthermore, we investigated the expression of collagen type I and X which specifically appears in bony calcified structures. mRNA and protein

expressions of collagen type I increased in young PACAP KO cartilage, and even stronger elevation was detected in aged PACAP KO joints (Fig. 6a, b). Collagen type X mRNA expression did not significantly alter, but dramatic protein expression elevation was detected in young PACAP KO mice (Fig. 6a, b). In aged PACAP KO joints, highly elevated mRNA and protein expression of collagen type X were detected (Fig. 6a, b). Location of collagen type

Fig. 3 Investigation of PACAP and its receptors in articular cartilage. mRNA (a) and protein (b) expression of preproPACAP, PAC1, VPAC1 and VPAC2 receptors of cartilage. For RT-PCR and Western blot reactions, actin was used as control. Optical signal density was measured and results were normalized to the WT controls. For a and b, numbers below signals represent integrated signal densities determined by ImageJ software. Asterisks indicate significant ($*p < 0.05$) alteration of expression compared to the respective control. Representative data of 5 independent experiments



X was followed by immunohistochemistry. In young WT mice, almost undetectable amount of collagen type X was shown in articular cartilage, while subchondral bone showed normal immunopositivity (Fig. 6c). In PACAP KO young animals, intensified immunopositivity was identified in subchondral bone and increased positivity was visible in articular cartilage (Fig. 6c). Both in WT and PACAP KO-aged mice, strong signal was detected in the

subchondral region; moreover, strong collagen type X positivity appeared around the chondrons of articular cartilage (Fig. 6c).

Discussion

In the present work, we demonstrated that genetical ablation of PACAP causes morphological and

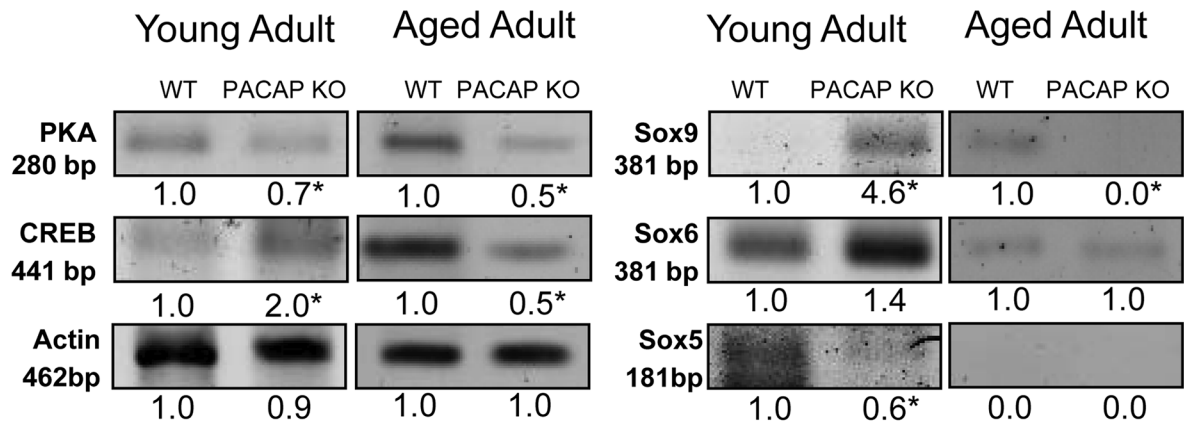
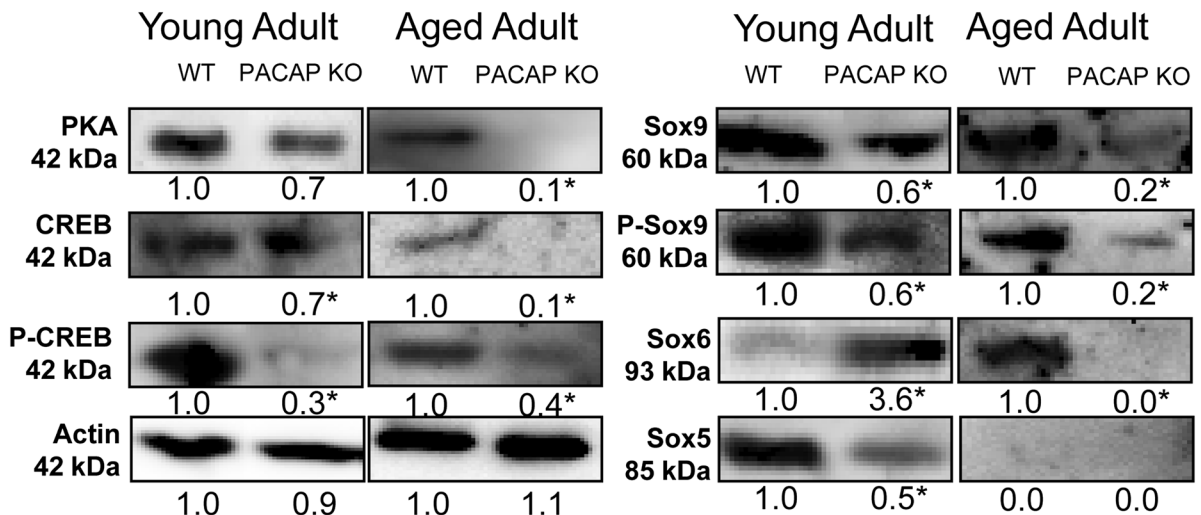
a RT-PCR**b Western blot**

Fig. 4 Investigation of canonical PACAP signaling in cartilage. mRNA (a) and protein (b) expression of PKA, CREB, Sox9, Sox6, and Sox5. For RT-PCR and Western blot reactions, actin was used as control. Optical signal density was measured and results were normalized to the WT controls. For **a** and **b**, numbers

below signals represent integrated signal densities determined by ImageJ software. Asterisks indicate significant ($*p < 0.05$) alteration of expression compared to the respective control. Representative data of 5 independent experiments

biochemical alterations in articular cartilage possibly turning this tissue more prone to degenerative diseases such as osteoarthritis (OA). Mature articular cartilage is an avascular and aneural tissue with a very low metabolic activity. Chondrocytes live in a milieu where they are exposed to acidic pH and low oxygen tension, and nutrients are transported to the cells by diffusion from the synovial fluid. Developing chondrocytes establish the specific zonal architecture of articular cartilage during foetal development (Zhang et al. 2012). Terminally differentiated hypertrophic chondrocytes secrete a cartilage matrix rich in collagen type X and the calcified

cartilage of hypertrophic zone in articular cartilage provides a biomechanical transition between hyaline cartilage and the subchondral bone (Mora et al. 2018). Biologically proper internal structure of articular cartilage is needed for the optimal weight bearing capability and joint function. Several signaling pathways contribute to the formation of collagen type II-rich ECM (Fodor et al. 2013; Juhasz et al. 2014c; Matta et al. 2008; Matta et al. 2011; Varga et al. 2011; Zakany et al. 2005; Zakany et al. 2002). In aging, the normal homeostasis of articular cartilage becomes shifted toward matrix degradation. Age related alterations of chondrocytes

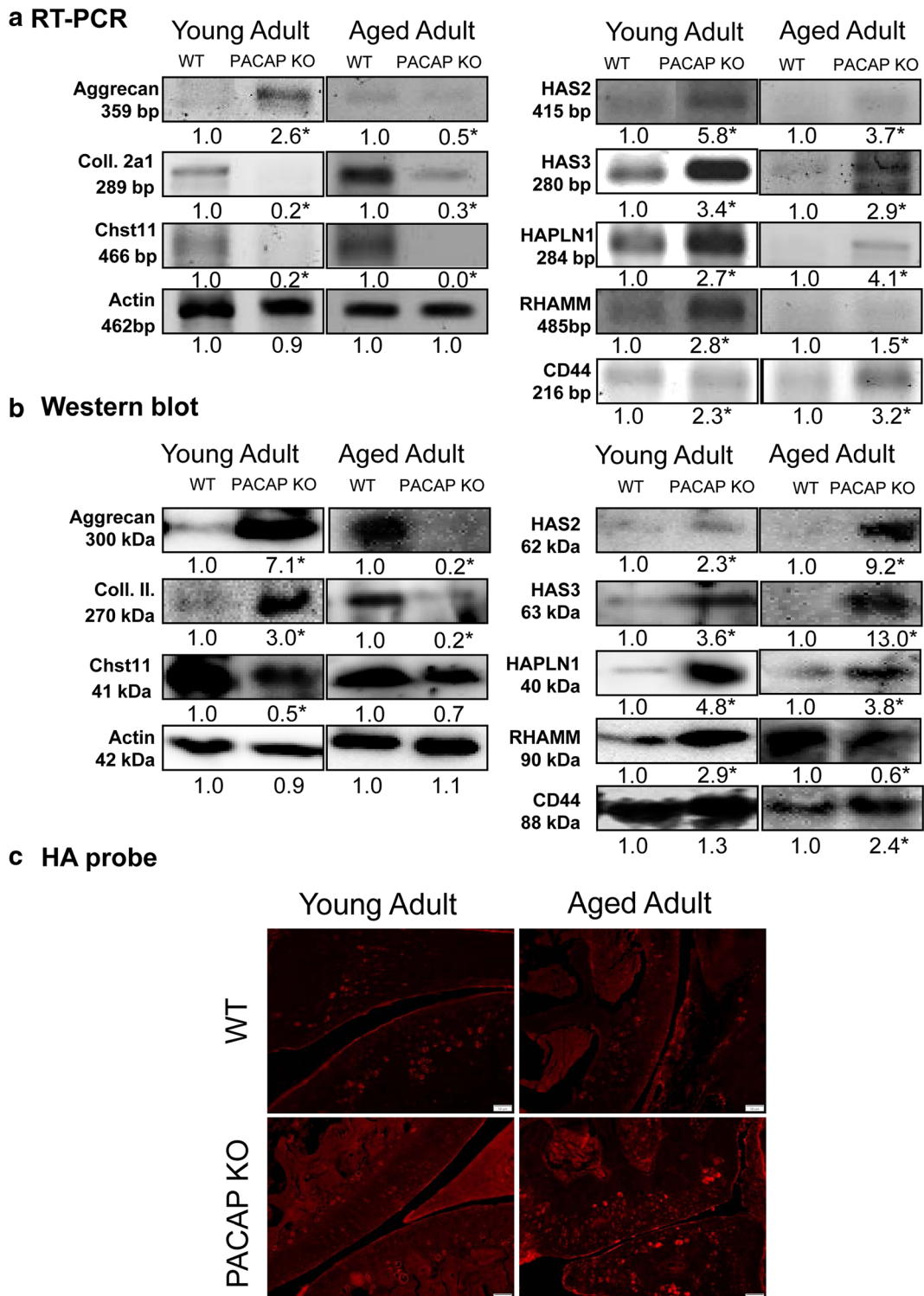


Fig. 5 ECM production in articular cartilage. **a** mRNA and **b** protein expressions of Aggrecane, collagen type II, HAPLN1, HAS2, HAS3, RHAMM and CD44 in articular cartilage. Actin was used as a control. Numbers below signals represent integrated signal densities determined by ImageJ software. Asterisks indicate

significant ($*p < 0.05$) alteration of expression compared to the respective control. **c** HA-binding probe in hyaline cartilage. Original magnification was $\times 20$. Scale bar: 50 μm . Representative data of 5 independent experiments

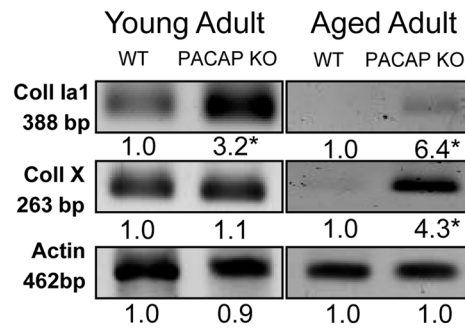
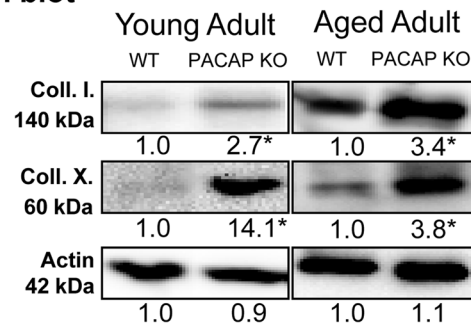
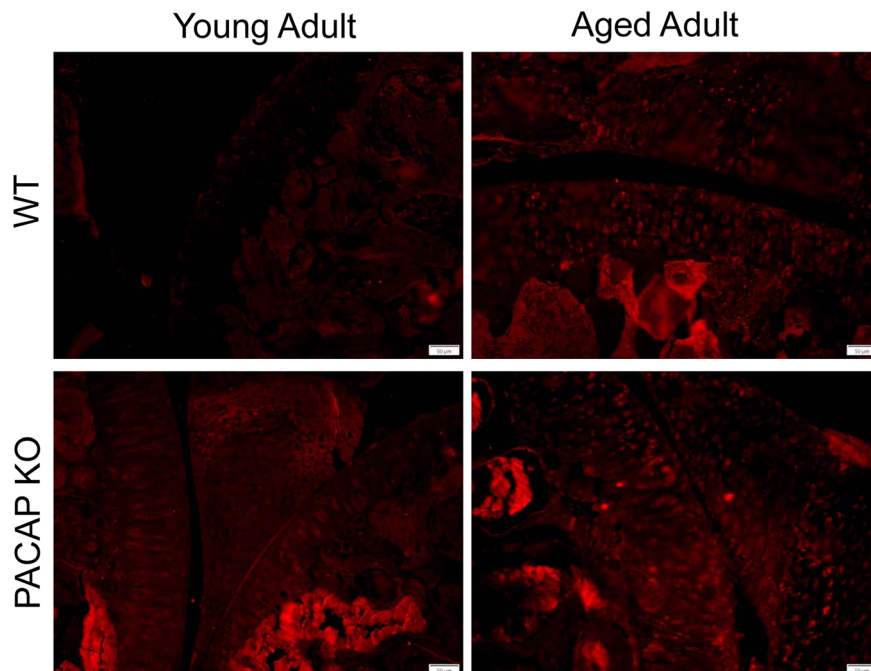
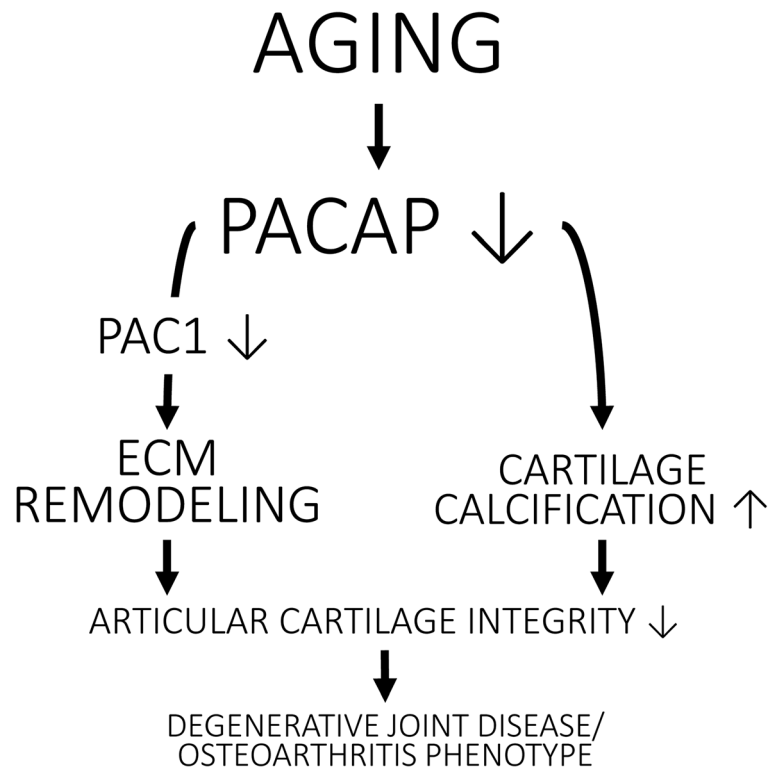
a RT-PCR**b Western blot****c Collagen type X immunohistochemistry**

Fig. 6 Collagen expression in cartilage. mRNA (**a**) and protein (**b**) expressions of collagen type I and X in cartilage. For RT-PCR and Western blot reactions, actin was used as controls. Numbers below signals represent integrated signal densities determined by ImageJ software. Asterisks indicate significant ($*p < 0.05$)

alteration of expression compared to the respective control. **c** Collagen type X immunohistochemistry in hyaline cartilage. Original magnification was $\times 20$. Scale bar: 50 μm . Representative data of 5 independent experiments

Fig. 7 PACAP function in aging. Concentration of PACAP and expression of PAC1 receptor reduce in aging process of articular cartilage. Reduction of the neuropeptide induces decreased cartilage remodeling but enhances the calcification processes of articular cartilage. Therefore, PACAP is important in maintaining cartilage integrity and prevents formation of pathological illnesses such as osteoarthritis



phenotype and signaling or remodeling disorders have been reviewed by Davies et al. (2017). Injury or overload of articular cartilage, particularly in elderly people, can induce OA (Bolduc et al. 2018) and when it develops, a progressive degradation of ECM may lead to a complete destruction of cartilage (Jimenez et al. 2018; Mora et al. 2018). Aging or OA-related matrix degradation of articular cartilage is hardly treatable; only few methods are used in the clinical practice such as advanced glycation end products (AGE) treatment (Satake et al. 2018) or corticosteroid injections (Mora et al. 2018). With these interventions, decrease of joint inflammation and conservation of the status of articular cartilage can be the main goal. Shifting aging-related cartilage alterations toward later life periods or modifying senescent chondrocytes can be another possibility (Hou et al. 2018; Jeon et al. 2018). Currently, stem cell therapy seems an emerging method for prevention both of the age-related cartilage degradation and OA formation (Krajewska-Wlodarczyk et al. 2018).

PACAP was found to exert protecting effects in different tissues. It can be beneficial in treatments of retinopathy (Szabadfi et al. 2016), Parkinson's disease (Brown et al. 2014) and ischemia (Reglodi et al. 2018d). It is also known that PACAP induces the activation of

anti-apoptotic processes and leads to decreases of pro-apoptotic factors (Reglodi et al. 2018a). Deficient PACAP-signaling was found in various neurodegenerative diseases such as Alzheimer's disease (Wu et al. 2006) and Parkinson's disease (Feher et al. 2018). Furthermore, reduced metabolism is detected in aging process (LaRoche et al. 2018; Nacarelli et al. 2018; Tian et al. 2017) which can be compensated by PACAP (Mansouri et al. 2016). Aging can lead to several skeletal and oral diseases such as dental root caries or alveolar bone loss (An et al. 2018); on the other hand, PACAP regulates the development of teeth (Fulop et al. 2018). Regarding cartilage and bone development and disease models, our group previously described that PACAP has a positive effect on chondrogenesis with the elevation of Sox9 activation (Juhasz et al. 2014a) and prevents the harmful effects of oxidative stress and mechanical overload in *in vitro* chondrogenesis (Juhasz et al. 2014a; Juhasz et al. 2015b). The presence of PACAP receptors in hyaline cartilage was demonstrated in chicken high density chondrifying cell cultures (Juhasz et al. 2014a) and in human OA (Giunta et al. 2015). Furthermore, the addition of PACAP influenced the expression of ECM molecules, such as HA (Juhasz et al. 2014a) or collagens (Juhasz et al. 2015b). The lack

of PACAP resulted in a signaling disorder femur development (Jozsa et al. 2018). Although the importance of PACAP-signaling and its positive role in OA is likely (Grassel and Muschter 2018), the role of PACAP in pathogenesis of cartilage disorders is not extensively studied and no information is available about its function in cartilage aging.

It is known that increased thickness of calcified cartilage can be detected in hip joints in early stages of OA (Hartlev et al. 2018). In knee joints of aged PACAP KO mice, significant thickening of articular cartilage and subchondral bone, along with decreased metachromasia, was our most obvious histological observation. This increase was parallel with disturbed ratio of the various components in the ECM. In aged PACAP KO animals, more collagen type I, elevated HA content was detected along with decrease of aggrecan and type II collagen. Loss of aggrecan was also proved by reduced metachromasia with DMMB. Altogether, these alterations can lead to softening of the articular cartilage which could induce thickening of subchondral bone. These microscopic morphological changes seem very similar to initial stages of OA (Lahm et al. 2017). It also suggests that the neuropeptide is involved in the inhibition of articular cartilage aging by maintaining chondrocyte plasticity (Varela-Eirin et al. 2018).

Along with aging, loss of PAC1 receptor was detected in articular cartilage of PACAP KO mice, which can be a factor triggering an ECM formation disorder (Fig. 7). This finding further supports the importance of PAC1 receptor activation in cartilage differentiation and proper ECM synthesis (Juhasz et al. 2014a). Similarly, PAC1 receptor reduction was also shown in retinal aging of PACAP KO mice (Kovacs-Valasek et al. 2017), although elevation was detected in young gene deficient mice. This further strengthens the hypothesis that presence of PACAP receptors exerts tissue-specific effects during aging (Reglodi et al. 2018b). VPAC1 receptor expression was identified in articular cartilage, its expression was almost undetectably low, suggesting that PAC1 is the dominant receptor in this tissue (Juhasz et al. 2014a).

Although the expression of PKA is not PACAP-dependent, we detected reduced PKA expression in aged PACAP gene-deficient mice. As PKA phosphorylates CREB and Sox9 transcription factors, this observation can explain the decreased activation and expression of these transcription factors. Reduced phosphorylation of CREB and Sox9 was more pronounced in aged articular cartilage (Zhang et al. 2016). We have

described earlier that activation of Sox9 also depends on PAC1 receptor activation (Juhasz et al. 2014a), and the lack of the neuropeptide further decreased the Sox9-dependent aggrecan and collagen expression (Zhang et al. 2016). These results suggest that the presence of PACAP is necessary for maintenance of continuous activation of Sox9 to produce and maintain the cartilage specific matrix expression. Sox5 and Sox6 are also positive regulators of chondrogenesis (Nishimura et al. 2018), and the lack of PACAP reduces the expression of Sox5 but elevates Sox6 expression. It seems that the reduced Sox9 expression is compensated in the lack of the neuropeptide by the elevated Sox6 expression in articular cartilage of young adults. A very similar phenomenon was identified in testis of PACAP KO mice, where the decreased Sox9 expression was compensated by an elevated Sox10 production (Reglodi et al. 2018c). Sox6 elevation resulted in the increase of aggrecan and collagen type II expression in young PACAP gene-deficient mice, accounting for the normal cartilage morphology. Similar compensatory mechanisms were identified in teeth of PACAP KO mice by the activation of Notch signaling (Fulop et al. 2018) or in femurs where augmented BMP signaling normalized the bone formation (Jozsa et al. 2018). Sox5 and Sox6 play important roles in the formation of proper articular cartilage morphology during development (Dy et al. 2010), but Sox5 function is diminished in aging process. Although Sox6 is detectable in aged WT mice, it is not present in PACAP KO animals. The decreased expression of Sox6 resulted in the loss of compensatory mechanism and further reduced aggrecan and collagen type II expression leading to the structural disorder of ECM in articular cartilage of PACAP gene-deficient mice. Moreover, lowered transferase (Chst11) expression can be the explanation of the decreased presence of sulphated glycosaminoglycans which was shown by a paler metachromasia in aged PACAP KO mice. Sox9, Sox5 and Sox6 are the major transcription factors of chondrogenesis, and their activation results various gene activations (Akiyama and Lefebvre 2011). Here we gave evidence that PACAP-signaling plays an essential role in Sox9 and Sox5 function, but Sox6, at least, partly was PACAP independently activated and compensated the lowered function of Sox9 and Sox5 in young PACAP KO mice. Our results suggest that the activation of Sox transcription factors is age dependent and in case of Sox9 this was demonstrated previously (Zhang et al. 2016). We observed that the absence of PACAP further

reduced Sox9 and Sox5 function, and it further strengthens the hypothesis that PACAP can keep balancing in crosstalks of various signaling pathways even during aging of tissues (Fig. 7) (Jozsa et al. 2018; Niewiadomski et al. 2013; Szentleky et al. 2019).

Interestingly, the thickness of articular cartilage increases in aging PACAP KO mice; therefore, we analysed the HA homeostasis of hyaline cartilage. Expression of HAS-ses and HA-binding proteins and receptors such as HAPLN1 and CD44 increases in young and aged PACAP KO mice. Furthermore, the presence of HA is elevated in the articular cartilage during aging. Coincidentally, in aged synovial cavity, decreased expression of HA was detected (Temple-Wong et al. 2016). Increased serum HA level was shown in aged population which can be a diagnostic sign of OA (Inoue et al. 2011). Moreover, aggrecanase can induce the HA release from aged articular cartilage which can enhance the destruction of the cartilage matrix during degenerative joint diseases such as OA (Chockalingam et al. 2004). Increased MMP activity was detected in the ECM of cardiac muscle tissue during aging (Meschiari et al. 2017), but we showed a PACAP-dependent reduction of MMPs in mechanical overload of chondrogenic cell cultures (Szentleky et al. 2019). RHAMM is an intracellular HA-binding receptor which can be activated by ERK (Katona et al. 2016). Its expression is reduced in aged PACAP KO animals, suggesting that intracellular HA function is decreased as it was demonstrated in skin aging (Tzello et al. 2009). Therefore, the appearance of HA around the chondrons can reflect on imbalanced HA distribution and may be a sign of ECM degradation in PACAP KO knee joints. Previously, we demonstrated that PACAP addition resulted in a reduced expression of hyaluronidases and aggrecanases in stress reactions (Szentleky et al. 2019). We suppose that chondrocytes cannot precisely control aggrecanase activation in PACAP KO mice. In aged cartilage, the elevated aggrecanase activity is proven to trigger HA release into the synovial cavity. Our results indicate that PACAP is a key molecule in maintaining cartilage matrix and keeping the balance between matrix production and degradation (Fig. 7) (Juhász et al. 2015b; Szentleky et al. 2019). Furthermore, the absence of PACAP probably triggers an early aging process which shows the characteristic signs of OA (Fig. 7).

In addition, we also detected increased expression and presence of collagen type I and X in aged articular cartilages. The expression of these collagens is stronger in PACAP gene-deficient mice. In intervertebral disc degradation an increased collagen type X was shown (Hristova

et al. 2011) or age related elevation of collagen type X was demonstrated in bone and ligament healing (Wang et al. 2006). Furthermore, aging induced the expression elevation of collagen type I and X in mandibular condylar cartilage (Inoue et al. 2002). We also published that addition of PACAP can induce the normalization of collagen type X expression in mechanical overload (Juhász et al. 2015b). Additionally, PACAP deficiency increased collagen type I expression in femurs (Jozsa et al. 2018). According to our previous results, PACAP can act on cartilage ECM structure via activation hedgehog signaling (Juhász et al. 2015b). The absence of PACAP disturbs signaling crosstalks of hedgehog activation, subsequently augments the expression of bone-specific collagen expressions and enhances cartilage matrix calcification. These findings further confirm that the lack of PACAP triggers an accelerated cartilage aging and the appearance of non-specific collagens in cartilage may cause OA-like cartilage matrix formation (Fig. 7).

In conclusion, we provided evidence that PACAP has an important function in proper cartilage matrix production in young animals as it seems to keep the balance between matrix production and matrix degradation (Fig. 7). The lack of the neuropeptide disturbs normal ECM composition of articular cartilage leading to early signs of aging in this tissue, which ultimately can cause a degenerative joint disease (Fig. 7).

Acknowledgements The authors are grateful for Mrs. Krisztina Biró for excellent technical assistance.

Author contributions Study conception and design: T J, D R, V Sz, B B, S T, V Sz, J V and T J performed the molecular biological analysis. V Sz and H P were responsible for the DMMB and HE staining. B F and A J were responsible for the animal care and removing the limbs. Geometric analysis were performed by B B. Acquisition of data: V Sz, B F, A T. Analysis and interpretation of data: V Sz, B B, T J, H P, A J, A T, R Z, D R. Participated in drafting the manuscript: V Sz, S T, R Z, T J, D R

Funding information Open access funding provided by University of Debrecen (DE). NKFIK115874, K119759, NKFIHFK129190, PTE AOK Research Grant, MTA-TKI 14016, GINOP-2.3.2-15-2016-00050 “PEPSYS”, New National Excellence Program of the Ministry of Human Capacities (UNKP-16-4-IV.), 2017-1.2.1-NKP-2017-00002 Nemzeti Agykutatási Program EFOP-3.6.1.-16-2016-00004 Comprehensive Development for Implementing Smart Specialization Strategies at the University of Pécs, EFOP-3.6.2-16-2017-00008 “The role of neuro-inflammation in neurodegeneration: from molecules to clinics”, Centre for Neuroscience of the University of Pécs, EFOP-3.6.3-VEKOP-16-2017-00009, University of Debrecen (OTKA Bridging Fund), EFOP-3.6.1.-16-2016-00004 Comprehensive Development for

Implementing Smart Specialization Strategies at the University of Pécs (Budapest, Hungary), NAP 2017-1.2.1-NKP-2017-00002 and OTKA-NN 114458. The project is co-financed by the European Union and the European Social Fund. Bolyai Janos Research Scholarship (J.T., A.T.). Szodoray Lajos and Magyary Zoltán Funds by Hungarian Academy of Science and the European Union and the State of Hungary, co-financed by the European Social Funding. Fund in the framework of TÁMOP 4.2.4 (J.T.). A/2-11-1-2012-0001 “National Excellence Program”. Higher Education Institutional Excellence Program of the Ministry of Human Capacities FIKP.

Compliance with ethical standards All procedures were performed in accordance with the ethical guidelines approved by the University of Pécs (permission number: BA02/2000-15024/2011).

Competing interests The authors declare that there are no competing interests.

Open Access This article is distributed under the terms of the Creative Commons Attribution 4.0 International License (<http://creativecommons.org/licenses/by/4.0/>), which permits unrestricted use, distribution, and reproduction in any medium, provided you give appropriate credit to the original author(s) and the source, provide a link to the Creative Commons license, and indicate if changes were made.

References

- Akiyama H, Lefebvre V (2011) Unraveling the transcriptional regulatory machinery in chondrogenesis. *J Bone Miner Metab* 29:390–395. <https://doi.org/10.1007/s00774-011-0273-9>
- An JY, Darveau R, Kaeberlein M (2018) Oral health in geroscience: animal models and the aging oral cavity. *GeroScience* 40:1–10. <https://doi.org/10.1007/s11357-017-0004-9>
- Antons J, Marascio MGM, Nohava J, Martin R, Applegate LA, Bourban PE, Pioletti DP (2018) Zone-dependent mechanical properties of human articular cartilage obtained by indentation measurements. *J Mater Sci Mater Med* 29:57. <https://doi.org/10.1007/s10856-018-6066-0>
- Bolduc JA, Collins JA, Loeser RF (2018) Reactive oxygen species, aging and articular cartilage homeostasis. *Free Radic Biol Med*. <https://doi.org/10.1016/j.freeradbiomed.2018.08.038>
- Brown D, Tamas A, Reglodi D, Tizabi Y (2014) PACAP protects against inflammatory-mediated toxicity in dopaminergic SH-SY5Y cells: implication for Parkinson’s disease. *Neurotox Res* 26:230–239. <https://doi.org/10.1007/s12640-014-9468-x>
- Chockalingam PS, Zeng W, Morris EA, Flannery CR (2004) Release of hyaluronan and hyaladherins (aggrecan G1 domain and link proteins) from articular cartilage exposed to ADAMTS-4 (aggrecanase 1) or ADAMTS-5 (aggrecanase 2). *Arthritis Rheum* 50:2839–2848. <https://doi.org/10.1002/art.20496>
- Davies JMS, Cillard J, Friguet B, Cadenas E, Cadet J, Cayce R, Fishmann A, Liao D, Bulteau AL, Derbré F, Rébillard A, Burstein S, Hirsch E, Kloner RA, Jakowec M, Petzinger G, Sauce D, Sennlaub F, Limon I, Jursini F, Maiorino M, Economides C, Pike CJ, Cohen P, Salvayre AN, Halliday MR, Lundquist AJ, Jakowec NA, Mechta-Grigoriou F, Mericskay M, Mariani J, Li Z, Huang D, Grant E, Forman HJ, Finch CE, Sun PY, Pomatto LCD, Agbulut O, Warburton D, Neri C, Rouis M, Cillard P, Capeau J, Rosenbaum J, Davies KJA (2017) The oxygen paradox, the French paradox, and age-related diseases. *Geroscience* 39(5–6):499–550
- Dy P et al (2010) Synovial joint morphogenesis requires the chondrogenic action of Sox5 and Sox6 in growth plate and articular cartilage. *Dev Biol* 341:346–359. <https://doi.org/10.1016/j.ydbio.2010.02.024>
- Feher M, Gaszner B, Tamas A, Gil-Martinez AL, Fernandez-Villalba E, Herrero MT, Reglodi D (2018) Alteration of the PAC1 receptor expression in the basal ganglia of MPTP-induced parkinsonian macaque monkeys. *Neurotox Res* 33:702–715. <https://doi.org/10.1007/s12640-017-9841-7>
- Fodor J et al (2013) Store-operated calcium entry and calcium influx via voltage-operated calcium channels regulate intracellular calcium oscillations in chondrogenic cells. *Cell Calcium* 54:1–16. <https://doi.org/10.1016/j.ceca.2013.03.003>
- Fulop BD et al (2018) Altered Notch signaling in developing molar teeth of pituitary adenylate cyclase-activating polypeptide (PACAP)-deficient mice. *J Mol Neurosci*. <https://doi.org/10.1007/s12031-018-1146-7>
- Giunta S, Castorina A, Marzagalli R, Szychlinska MA, Pichler K, Mobasheri A, Musumeci G (2015) Ameliorative effects of PACAP against cartilage degeneration. Morphological, immunohistochemical and biochemical evidence from in vivo and in vitro models of rat osteoarthritis. *Int J Mol Sci* 16:5922–5944. <https://doi.org/10.3390/ijms16035922>
- Gourlet P, Vandermeers A, Vertongen P, Rathe J, de Neef P, Cnudde J, Waelbroeck M, Robberecht P (1997) Development of high affinity selective VIP1 receptor agonists. *Peptides* 18:1539–1545
- Grassel S, Muschter D (2018) Do neuroendocrine peptides and their receptors qualify as novel therapeutic targets in osteoarthritis? *Int J Mol Sci* 19. <https://doi.org/10.3390/ijms19020367>
- Hartlev LB, Klose-Jensen R, Thomsen JS, Nyengaard JR, Boel LWT, Laursen MB, Laurberg TB, Nielsen AW, Steengaard-Pedersen K, Hauge EM (2018) Thickness of the bone-cartilage unit in relation to osteoarthritis severity in the human hip joint RMD open 4:e000747 doi:<https://doi.org/10.1136/rmdopen-2018-000747>
- Hashimoto H et al (2001) Altered psychomotor behaviors in mice lacking pituitary adenylate cyclase-activating polypeptide (PACAP). *Proceedings of the National Academy of Sciences of the United States of America*. 98:13355–13360. <https://doi.org/10.1073/pnas.231094498>
- Hou A et al (2018) Cellular senescence in osteoarthritis and anti-aging strategies. *Mech Ageing Dev* 175:83–87. <https://doi.org/10.1016/j.mad.2018.08.002>
- Hristova GI, Jarzem P, Ouellet JA, Roughley PJ, Epure LM, Antoniou J, Mwale F (2011) Calcification in human intervertebral disc degeneration and scoliosis. *J Orthop Res* 29:1888–1895. <https://doi.org/10.1002/jor.21456>
- Inoue H, Hiraki Y, Nawa T, Ishizeki K (2002) Phenotypic switching of in vitro mandibular condylar cartilage during matrix mineralization. *Anat Sci Int* 77:237–246. <https://doi.org/10.1046/j.0022-7722.2002.00031.x>
- Inoue R et al (2011) Knee osteoarthritis, knee joint pain and aging in relation to increasing serum hyaluronan level in the

- Japanese population. *Osteoarthr Cartil* 19:51–57. <https://doi.org/10.1016/j.joca.2010.10.021>
- Ivic I et al (2017) Aging-induced modulation of pituitary adenylate cyclase-activating peptide- and vasoactive intestinal peptide-induced vasomotor responses in the arteries of mice. *J Vasc Res* 54:359–366. <https://doi.org/10.1159/000481781>
- Jeon OH, David N, Campisi J, Elisseeff JH (2018) Senescent cells and osteoarthritis: a painful connection. *J Clin Invest* 128:1229–1237. <https://doi.org/10.1172/JCI95147>
- Jimenez G, Cobo-Molinos J, Antich C, Lopez-Ruiz E (2018) Osteoarthritis: trauma vs disease. *Adv Exp Med Biol* 1059:63–83. https://doi.org/10.1007/978-3-319-76735-2_3
- Jozsa G et al (2018) Signalling alterations in bones of pituitary adenylate cyclase activating polypeptide (PACAP) gene deficient mice. *Int J Mol Sci* 19. <https://doi.org/10.3390/ijms19092538>
- Juhasz T et al (2014a) Pituitary adenylate cyclase activating polypeptide (PACAP) signalling exerts chondrogenesis promoting and protecting effects: implication of calcineurin as a downstream target. *PLoS One* 9:e91541. <https://doi.org/10.1371/journal.pone.0091541>
- Juhasz T et al (2014b) Pituitary adenylate cyclase-activating polypeptide (PACAP) signalling enhances osteogenesis in UMR-106 cell line. *J Mol Neurosci* 54:555–573. <https://doi.org/10.1007/s12031-014-0389-1>
- Juhasz T et al (2014c) Mechanical loading stimulates chondrogenesis via the PKA/CREB-Sox9 and PP2A pathways in chicken micromass cultures. *Cell Signal* 26:468–482. <https://doi.org/10.1016/j.cellsig.2013.12.001>
- Juhasz T, Helgadottir SL, Tamas A, Reglodi D, Zakany R (2015a) PACAP and VIP signaling in chondrogenesis and osteogenesis. *Peptides* 66:51–57. <https://doi.org/10.1016/j.peptides.2015.02.001>
- Juhasz T et al (2015b) Pituitary adenylate cyclase activating polypeptide (PACAP) pathway is induced by mechanical load and reduces the activity of hedgehog signaling in chondrogenic micromass cell cultures. *Int J Mol Sci* 16:17344–17367. <https://doi.org/10.3390/ijms160817344>
- Katona E et al (2016) PP2B and ERK1/2 regulate hyaluronan synthesis of HT168 and WM35 human melanoma cell lines. *Int J Oncol* 48:983–997. <https://doi.org/10.3892/ijo.2015.3313>
- Kovacs-Valasek A et al (2017) Accelerated retinal aging in PACAP knock-out mice. *Neuroscience* 348:1–10. <https://doi.org/10.1016/j.neuroscience.2017.02.003>
- Krajewska-Wlodarczyk M, Owczarczyk-Saczonek A, Placek W, Osowski A, Wojtkiewicz J (2018) Articular cartilage aging-potential regenerative capacities of cell manipulation and stem cell therapy. *Int J Mol Sci* 19. <https://doi.org/10.3390/ijms19020623>
- Laasanen MS, Töyräs J, Korhonen RK, Rieppo J, Saarakkala S, Nieminen MT, Hirvonen J, Jurvelin JS (2003) Biomechanical properties of knee articular cartilage. *Biorheology* 40:133–140
- Lahm A, Dabravolski D, Spank H, Merk H, Esser J, Kasch R (2017) Regional differences of tibial and femoral cartilage in the chondrocyte gene expression, immunohistochemistry and composite in different stages of osteoarthritis. *Tissue Cell* 49:249–256. <https://doi.org/10.1016/j.tice.2017.02.004>
- LaRoche DP, Melanson EL, Baumgartner MP, Bozzuto BM, Libby VM, Marshall BN (2018) Physiological determinants of walking effort in older adults: should they be targets for physical activity intervention? *GeroScience* 40:305–315. <https://doi.org/10.1007/s11357-018-0032-0>
- Lefebvre V, Behringer RR, de Crombrughe B (2001) L-Sox5, Sox6 and Sox9 control essential steps of the chondrocyte differentiation pathway. *Osteoarthr Cartil* 9(Suppl A):S69–S75
- Li L, Duan X, Fan Z, Chen L, Xing F, Xu Z, Chen Q, Xiang Z (2018) Mesenchymal stem cells in combination with hyaluronic acid for articular cartilage defects. *Sci Rep* 8:9900. <https://doi.org/10.1038/s41598-018-27737-y>
- Liu CF, Lefebvre V (2015) The transcription factors SOX9 and SOX5/SOX6 cooperate genome-wide through super-enhancers to drive chondrogenesis. *Nucleic Acids Research*. 43:8183–8203. <https://doi.org/10.1093/nar/gkv688>
- Mansouri S, Lietzau G, Lundberg M, Nathanson D, Nystrom T, Patrone C (2016) Pituitary adenylate cyclase activating peptide protects adult neural stem cells from a hypoglycaemic milieu. *PLoS One* 11:e0156867. <https://doi.org/10.1371/journal.pone.0156867>
- Matta C, Fodor J, Szejgyarto Z, Juhasz T, Gergely P, Cserech L, Zakany R (2008) Cytosolic free Ca²⁺ concentration exhibits a characteristic temporal pattern during in vitro cartilage differentiation: a possible regulatory role of calcineurin in Ca-signalling of chondrogenic cells. *Cell Calcium* 44:310–323. <https://doi.org/10.1016/j.ceca.2007.12.010>
- Matta C et al (2011) PKCdelta is a positive regulator of chondrogenesis in chicken high density micromass cell cultures. *Biochimie* 93:149–159. <https://doi.org/10.1016/j.biochi.2010.09.005>
- Meschieri CA, Ero OK, Pan H, Finkel T, Lindsey ML (2017) The impact of aging on cardiac extracellular matrix. *GeroScience* 39:7–18. <https://doi.org/10.1007/s11357-017-9959-9>
- Miyata A, Arimura A, Dahl RR, Minamino N, Uehara A, Jiang L, Culler MD, Coy DH (1989) Isolation of a novel 38 residue-hypothalamic polypeptide which stimulates adenylate cyclase in pituitary cells. *Biochem Biophys Res Commun* 164:567–574
- Mora JC, Przkora R, Cruz-Almeida Y (2018) Knee osteoarthritis: pathophysiology and current treatment modalities. *J Pain Res* 11:2189–2196. <https://doi.org/10.2147/JPR.S154002>
- Nacarelli T, Azar A, Altinok O, Orynbayeva Z, Sell C (2018) Rapamycin increases oxidative metabolism and enhances metabolic flexibility in human cardiac fibroblasts. *GeroScience*. <https://doi.org/10.1007/s11357-018-0030-2>
- Niewiadomski P, Zhujiang A, Youssef M, Waschek JA (2013) Interaction of PACAP with Sonic hedgehog reveals complex regulation of the hedgehog pathway by PKA. *Cell Signal* 25:2222–2230. <https://doi.org/10.1016/j.cellsig.2013.07.012>
- Nishimura R, Hata K, Nakamura E, Murakami T, Takahata Y (2018) Transcriptional network systems in cartilage development and disease *Histochem Cell Biol* 149:353–363 doi: <https://doi.org/10.1007/s00418-017-1628-7>
- Poulet B, Staines KA (2016) New developments in osteoarthritis and cartilage biology *Curr Opin Pharmacol* 28:8–13 doi: <https://doi.org/10.1016/j.coph.2016.02.009>
- Redondo ML, Naveen NB, Liu JN, Tauro TM, Southworth TM, Cole BJ (2018) Preservation of knee articular cartilage *Sports Med Arthrosc Rev* 26:e23–e30 doi:<https://doi.org/10.1097/JSA.0000000000000226>
- Reglodi D, Atlasz T, Jungling A, Szabo E, Kovari P, Manavalan S, Tamas A (2018a) Alternative routes of administration of the

- neuroprotective pituitary adenylate cyclase activating polypeptide. *Curr Pharm Des.* <https://doi.org/10.2174/1381612824666181112110934>
- Reglodi D et al (2018b) PACAP deficiency as a model of aging. *GeroScience.* <https://doi.org/10.1007/s11357-018-0045-8>
- Reglodi D et al (2018c) Disturbed spermatogenic signaling in pituitary adenylate cyclase activating polypeptide-deficient mice. *Reproduction* 155:129–139. <https://doi.org/10.1530/REP-17-0470>
- Reglodi D, Vaczy A, Rubio-Beltran E, MaassenVanDenBrink A (2018d) Protective effects of PACAP in ischemia J Headache Pain 19:19 doi:<https://doi.org/10.1186/s10194-018-0845-3>
- Sandor B et al (2014) Structural and morphometric comparison of the molar teeth in pre-eruptive developmental stage of PACAP-deficient and wild-type mice. *J Mol Neurosci* 54: 331–341. <https://doi.org/10.1007/s12031-014-0392-6>
- Satake Y, Takahashi K, Saito M, Takai S (2018) Objective colorimetric evaluation of aging-related articular cartilage degeneration. *J Nippon Med School* 85:157–165. https://doi.org/10.1272/jnms.JNMS.2018_85-23
- Szabadi K et al (2016) Pituitary adenylate cyclase activating polypeptide, a potential therapeutic agent for diabetic retinopathy in rats: focus on the vertical information processing pathway. *Neurotox Res* 29:432–446. <https://doi.org/10.1007/s12640-015-9593-1>
- Szentleky E et al (2019) Pituitary adenylate cyclase activating polypeptide (PACAP) reduces oxidative and mechanical stress-evoked matrix degradation in chondrifying cell cultures. *Int J Mol Sci* 20. <https://doi.org/10.3390/ijms20010168>
- Temple-Wong MM, Ren S, Quach P, Hansen BC, Chen AC, Hasegawa A, D’Lima DD, Koziol J, Masuda K, Lotz MK, Sah RL (2016) Hyaluronan concentration and size distribution in human knee synovial fluid: variations with age and cartilage degeneration. *Arthritis Res Ther* 18:18. <https://doi.org/10.1186/s13075-016-0922-4>
- Tian Q et al (2017) RHEB1 insufficiency in aged male mice is associated with stress-induced seizures. *GeroScience* 39: 557–570. <https://doi.org/10.1007/s11357-017-9997-3>
- Tzellos TG et al (2009) Extrinsic ageing in the human skin is associated with alterations in the expression of hyaluronic acid and its metabolizing enzymes. *Exp Dermatol* 18:1028–1035. <https://doi.org/10.1111/j.1600-0625.2009.00889.x>
- Varela-Eirin M, Loureiro J, Fonseca E, Corrochano S, Caeiro JR, Collado M, Mayan MD (2018) Cartilage regeneration and ageing: targeting cellular plasticity in osteoarthritis. *Ageing Res Rev* 42:56–71. <https://doi.org/10.1016/j.arr.2017.12.006>
- Varga Z et al (2011) Switch of voltage-gated K⁺ channel expression in the plasma membrane of chondrogenic cells affects cytosolic Ca²⁺-oscillations and cartilage formation. *PLoS One* 6:e27957. <https://doi.org/10.1371/journal.pone.0027957>
- Vaudry D et al (2009) Pituitary adenylate cyclase-activating polypeptide and its receptors: 20 years after the discovery. *Pharmacol Rev* 61:283–357. <https://doi.org/10.1124/pr.109.001370>
- Wang IE, Mitroo S, Chen FH, Lu HH, Doty SB (2006) Age-dependent changes in matrix composition and organization at the ligament-to-bone insertion. *J Orthop Res* 24:1745–1755. <https://doi.org/10.1002/jor.20149>
- Wu ZL, Ciallella JR, Flood DG, O’Kane TM, Bozyczko-Coyne D, Savage MJ (2006) Comparative analysis of cortical gene expression in mouse models of Alzheimer’s disease. *Neurobiol Aging* 27:377–386. <https://doi.org/10.1016/j.neurobiolaging.2005.02.010>
- Zakany R et al (2001) Okadaic acid-induced inhibition of protein phosphatase 2A enhances chondrogenesis in chicken limb bud micromass cell cultures. *Anat Embryol* 203:23–34
- Zakany R et al (2002) Protein phosphatase 2A is involved in the regulation of protein kinase A signaling pathway during in vitro chondrogenesis. *Exp Cell Res* 275:1–8. <https://doi.org/10.1006/excr.2002.5487>
- Zakany R et al (2005) Hydrogen peroxide inhibits formation of cartilage in chicken micromass cultures and decreases the activity of calcineurin: implication of ERK1/2 and Sox9 pathways. *Exp Cell Res* 305:190–199. <https://doi.org/10.1016/j.yexcr.2004.12.016>
- Zevenbergen L et al (2018) Cartilage-on-cartilage contact: effect of compressive loading on tissue deformations and structural integrity of bovine articular cartilage. *Osteoarthr Cartil.* <https://doi.org/10.1016/j.joca.2018.08.009>
- Zhang Y, Wang F, Tan H, Chen G, Guo L, Yang L (2012) Analysis of the mineral composition of the human calcified cartilage zone. *Int J Med Sci* 9:353–360. <https://doi.org/10.7150/ijms.4276>
- Zhang M, Lu Q, Miller AH, Barnhouse NC, Wang J (2016) Dynamic epigenetic mechanisms regulate age-dependent SOX9 expression in mouse articular cartilage. *Int J Biochem Cell Biol* 72:125–134. <https://doi.org/10.1016/j.biocel.2016.01.013>

Publisher’s note Springer Nature remains neutral with regard to jurisdictional claims in published maps and institutional affiliations.